Available online at www.sciencedirect.com
SCIENCE DIRECT®
Surface Science 588 (2005) 1–5
SURFACE SCIENCE
www.elsevier.com/locate/susc

Angular dependence of the sputtering yield of water ice by 100 keV proton bombardment

R.A. Vidal *, B.D. Teolis, R.A. Baragiola

Laboratory for Atomic and Surface Physics, Engineering Physics, University of Virginia, Charlottesville, VA 22904, USA

Received 25 February 2005; accepted for publication 2 May 2005
Available online 31 May 2005

Abstract

We measured the total sputtering yield of amorphous water ice for 100 keV H^+ as a function of the projectile incidence angle, and the angular distribution of the ejected H_2O and O_2 molecules, using a quartz-crystal microbalance and mass spectrometry, respectively, at temperatures of 20 K and 100 K. The total sputtering yield follows a $\cos^{-f}\theta$ dependence, with $f \cong 1.3$, regardless of the irradiation temperature. This is explained by the action of fast binary δ-electrons that relocate the electronic energy deposited by the ion near the surface into the bulk of the material.

We found that the O_2 emission follows a cosine dependence, as expected from isotropic collision cascades or if transport of the oxygen to the surface is by thermal diffusion. In contrast, H_2O emission is more outward peaked than cosine, which could be attributed to the blocking of large angle emission by the transient crater formed during sputtering of multiple water molecules by a given projectile.

Keywords: Atom–solid interactions; Ion bombardment; Sputtering; Water

1. Introduction

Sputtering (desorption) of water ice can result from energy deposited by energetic ions, electrons or photons [1]. The topic is interesting because it represents the archetypical case of sputtering of molecular solids, and because of its application to astrophysics, where sputtering is a source of atmospheres around icy bodies [2]. In the case of ions, there are two mechanisms for energy deposition that can lead to sputtering: direct momentum transfer to the nuclei of the water molecule (nuclear or elastic sputtering), and electronic transitions (ionizations and excitations) of water molecules followed by a, still unknown, mechanism that converts electronic energy into molecular motion.

* Corresponding author. Present address: INTEC, Güemes 3450, 3000 Santa Fe, Argentina. Tel.: +1 54 342 4559175; fax: +1 54 342 4550944.
E-mail address: rvidal@intec.unl.edu.ar (R.A. Vidal).

0039-6028/$ - see front matter © 2005 Elsevier B.V. All rights reserved.
doi:10.1016/j.susc.2005.05.007

Studies of sputtering of ice, spanning more than two decades, have been reviewed recently [1]. The main aspects are as follows. The sputtering yield Y (molecules/ion) peaks at the ion energy where the electronic stopping power (dE/dx) is maximum, around 90 keV for protons. In the electronic excitation regime Y increases sharply with the temperature of the ice above ~100 K and is independent of temperature below 100 K. The flux of sputtered species (ejecta) consists mainly of H_2O at low temperatures plus a small fraction of new molecules, H_2 and O_2. The sputtering of these synthesized molecules rises roughly exponentially with temperature, becoming an important contribution to the total sputtering yield above ~100 K.

For MeV light ions Brown et al. [3] found that the total sputtering yield does not depend on initial film thickness from 250 Å to 1.5 μm indicating that the erosion process is confined to a thin surface layer, and that erosion is not due to the escape of excited species from the entire track length. The situation is different for the sputtering of H_2 and O_2, which increase slightly with film thickness [4], indicating that processes deep in the film are contributing to the ejection, and which show a dependence of irradiation fluence, suggesting the participation of complex processes that may involve radicals.

There have been no experiments on the dependence of sputtering on the angle of ion incidence, or of the angular distribution of ejected molecules. This information is needed to understand the generation of atmospheres around icy bodies in the outer solar system. So far, modelers have used, as a proxy, the only data available for the dependence of sputtering on angle of incidence, θ, for solid CO [5] and O_2 [6] under MeV He^+ impact, where the sputtering yield is seen to vary as $\cos^{-f}\theta$ with $f \sim 1.6$. We thus undertook an effort to perform measurements of both angular dependences (incidence and emission angles) for the sputtering of water ice, both to obtain data useful for applications and because such new data might give information that can constrain possible mechanisms for the key and unknown processes of transformation of electronic excitation to atomic motion.

2. Experimental details

Experiments were performed in a cryopumped, stainless steel, ultrahigh vacuum chamber connected to a mass-analyzed 300 kV ion accelerator. The background pressure during the measurements was $\sim 1 \times 10^{-9}$ Torr, rising to $\sim 2 \times 10^{-9}$ Torr during the irradiations. A rotatable target assembly inside the chamber was cooled by a He cryostat that can reach temperatures close to 4 K. The target temperature was measured with a silicon diode to an accuracy of 1 K. Ice films were grown by vapor deposition on a 6 MHz gold-coated quartz-crystal microbalance that has a sensitivity of $\sim 10^{14}$ H_2O/cm^2 or about 0.1 monolayers. To grow amorphous ice films we effused high-purity isotopically labeled $H_2{}^{18}O$ water through a capillary array doser, perpendicularly onto the target crystal cooled to 100 K. The use of isotopically labeled $H_2{}^{18}O$ allowed us to detect $H_2{}^{18}O$ and $^{18}O_2$ over the H_2O and O_2 signals coming from the background in the vacuum system.

Total sputtering yields were determined from the measurements of the mass loss from the film, given by the frequency change of the crystal, and the measurement of the accumulated ion flux (fluence). We convert the mass loss measured by the microbalance to an equivalent number of water molecules/cm^2 and divide them by the number of incident particles/cm^2 to obtain the sputtering yield. This calculation takes into account the change of ion beam current density when the sample is tilted.

We analyzed the composition of the desorbed flux with two quadrupole mass spectrometers. Since the sputtered flux is essentially neutral (ejected ions constitute <1% of the ejected particles [4]), the QMS are operated with the electron impact ionizers turned on. An electron multiplier detector following the quadrupole mass selector improves the sensitivity by about two orders of magnitude. Partial sputtering fluxes (H_2O and O_2) correspond to the difference of the QMS signals with ion beam on and off. As shown in Fig. 1, one of the QMS (QMS 2) is at 270° relative to the ion beam direction. Since this instrument is not collimated it measures molecules after they

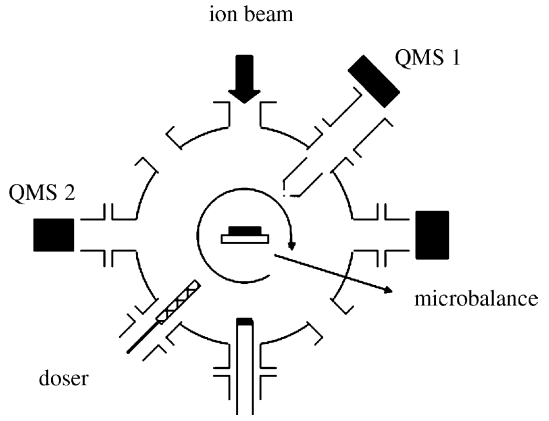

Fig. 1. Schematic diagram of apparatus.

have had many collisions with the chamber surfaces. Thus, the signal measured by QMS 2 is proportional to the total rate of ejection of molecules ejected from the ice film (and inversely proportional to the pumping speed, which is constant during the experiments). The other mass spectrometer, QMS 1, is at 45° relative to the ion beam direction and has a collimator that only allows measurement of molecules emitted in a narrow angular range (3.9°), with a negligible contribution from molecules that have bounced off other surfaces in the chamber. In addition, the axis of QMS 1 is at 90° off the line of view of the target, to prevent energetic particles such as reflected projectiles and fast sputtered atoms from hitting the quadrupole rods and the detector. Prior to taking this precaution we found a background at all masses, modulated by turning the ion beam on and off, which could be confused with a real signal.

To calculate $h(\varphi)$, the distribution of the sputtered particles vs. emission angle, φ, we make the assumption that it is independent of the angle of incidence of the projectile, θ, which is supported by the approximate symmetry of the distribution around φ. Thus, we can factor the angular distribution as

$$\mathrm{d}Y(\theta,\varphi) = g(\theta)\ h(\varphi)\,\mathrm{d}\Omega$$

where $\mathrm{d}Y(\theta,\varphi)$ is proportional to the signal measured by QMS 1 and $g(\theta)$ is proportional to that measured by QMS 2. The ratio of the signals from both QMSs is what we show later in this paper. The measurements were taken at saturation ion fluences ($>3\times10^{16}$ H^+/cm^2) to obviate complications due to the initial fluence dependence of O_2 emission [4].

3. Results and discussion

Fig. 2 shows the dependence of the total sputtering yield on incidence angle for 100 keV H^+ incident on a 1.8 μm water ice film at 100 K and 20 K. The results were fitted to a $\cos^{-f}\theta$ dependence which gave $f = 1.29 \pm 0.02$ (1.32 ± 0.05) for $T = 100$ K (20 K).

In Fig. 3 we show the angular distribution of the sputtered H_2O and O_2 for irradiation at 20 K and 100 K. It can be seen that the O_2 distribution is cosine while the H_2O distribution is more peaked forward than a cosine distribution. While for O_2 we do not see a temperature effect, within the limits of the experimental error, for H_2O we see a slight difference. The H_2O distribution follows a $\cos^n\varphi$ dependence with $n = 1.3 \pm 0.2$ at 100 K, and $n = 1.5 \pm 0.2$ at 20 K.

We now discuss the dependence of the sputtering yield on incidence angle θ as shown in Fig. 2.

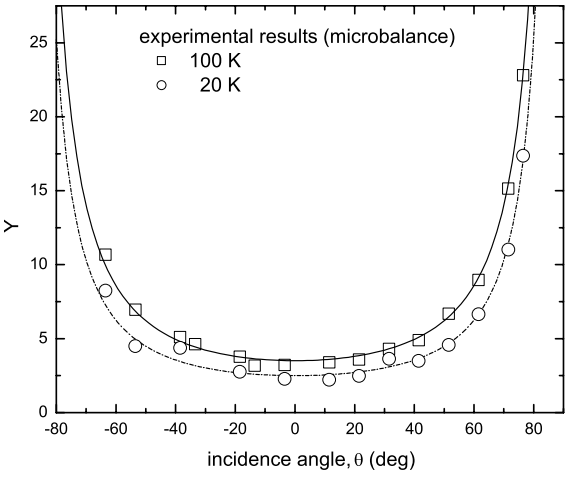

Fig. 2. Total sputtering yield (as measured using the quartz-crystal microbalance) as a function of the H^+ incidence angle for different temperatures: 20 K (circles), 100 K (squares). The lines are fits to $\cos^{-f}\theta$. $Y(20\text{ K}) = 2.5\cos^{-1.32}\theta$, $Y(100\text{ K}) = 3.5\cos^{-1.29}\theta$.

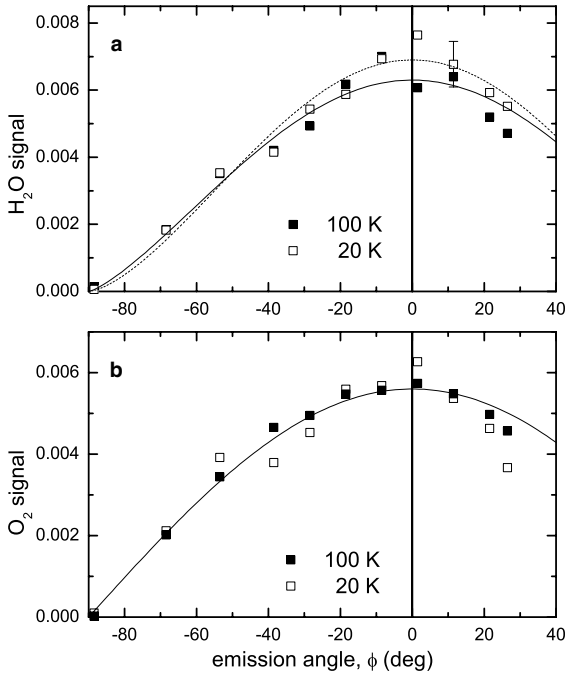

Fig. 3. Distribution of sputtered particles as a function of the emission angle, φ for two different irradiation temperatures, 100 K (full squares) and 20 K (open squares). The signals have been normalized so that the integral over the emission solid angle is equal to one. The lines are fits to $\cos^f\varphi$. (a) H_2O emission, 0.0063 $\cos^{1.3}\varphi$ fits to 100 K data (full line), 0.0069 $\cos^{1.5}\varphi$ fits to 20 K data (dashed line); (b) O_2 emission, 0.0056 cos φ (full line).

If the sputtering yield depended linearly on the energy lost by the projectile over the depth responsible for sputtering, Δ, it would vary as $\cos^{-1}\theta$ since the stopping power of the ion remains roughly constant over paths over 100 nm. An f value larger than 1 implies that E_D/E_L, the ratio of the energy deposited by the ion to the energy loss increases steeply with θ. $E_D < E_L$ since energetic secondary electrons (SE) can deposit their energy away from their point of origin. For instance, those SE excited close to the surface which are ejected do not deposit their energy in the ice, and the fast SE (so-called δ-electrons) have a forward peaked angular distribution since they are produced in binary collisions with the projectile [7]. This anisotropic angular distribution is responsible for the asymmetry in the electron emission yields from thin foils traversed by fast ions: the forward emission exceeds the backward emission by a factor that increases with ion velocity [8]. The effect tends to disappear at low projectile velocities when most of the binary electrons cannot produce further ionizations or have very small range.

The depth distribution of deposited energy has been used to model deviations from a $\cos^{-1}\theta$ dependence in electronic sputtering [9,10]. Here we propose a simple model for the effect of δ-electrons using the Sternglass parametric model [11] for the energy deposited along the ion track close to the surface:

$$dE_D/dx = dE/dx[1 - 1/2\exp(-x/L_\delta)] \quad (1)$$

where dE/dx is the average electronic stopping power over the sputtering depth Δ, L_δ is the decay constant of the forward relocation of the deposited energy by δ-electrons, x is measured along the ion track and $z = x\cos\theta$ is the depth. Sputtering is taken to be proportional to the integral of $(dE_D/dx)^2$ over Δ. The square dependence on dE_D/dx is based on the known proportionality of the sputtering yield with $(dE/dx)^2$ [1]. We found that a $\cos^{-f}\theta$ dependence with $f = 1.3$, that fits very closely to the experimental values, is obtained with $L_\delta/\Delta = 0.7$. For a typical δ-electron energy of ~100 eV, the most probable range of electrons in water is $L_\delta \sim 3$ nm [12] (for 218 eV, the energy of the most energetic δ-electrons produced by 100 keV protons, the range is ~8 nm). Thus, our procedure gives an estimate of the depth responsible for sputtering as $\Delta \sim 4$ nm.

We now turn to the angular distribution of sputtered molecules. A cosine distribution of emitted molecules, as observed for O_2, indicates either thermal desorption, or an isotropic cascade of recoils inside the solid [13]. On the other hand, the enhanced emission near the surface normal for H_2O indicates that the momentum distribution of recoils near the surface is peaked in the outward direction. A possible explanation is that during the sputtering of multiple water molecules in the narrow ion track, a transient crater is formed, in which the walls block the emission of molecules at large angles.

4. Conclusions

We obtained the dependence of sputtering of water ice on the angle of incidence of 100 keV protons, which are typical for the magnetospheres in the outer solar system. The $\cos^{-1.3}\theta$ dependence and the angular distribution of sputtered molecules can be used, together with previous measurements of energy distributions [14], to determine the escaping and gravitationally bound sputtered flux in different icy objects like satellites and ring particles. We suggest that the different angular distribution of ejected O_2 and H_2O molecules indicates a different excitation and transport mechanism for those molecules before they escape the solid.

Acknowledgments

We thank R.E. Johnson for useful comments. This research was supported by NSF Astronomy division, by NASA Planetary atmospheres program and by the NASA/JPL Cassini program under contract with SwRI.

References

[1] R.A. Baragiola, R.A. Vidal, W. Svendsen, J. Schou, M. Shi, D.A. Bahr, C.L. Atteberry, Nucl. Instrum. Meth. B 209 (2003) 294.
[2] M. Shi, R.A. Baragiola, D.E. Grosjean, R.E. Johnson, S. Jurac, J. Schou, J. Geophys. Res. 100 (1995) 26, 387.
[3] W.L. Brown, L.J. Lanzerotti, J.M. Poate, W.M. Augustyniak, Phys. Rev. Lett. 40 (1978) 1027.
[4] C.T. Reimann, J.W. Boring, R.E. Johnson, J.W. Garrett, K.R. Farmer, Surf. Sci. 147 (1984) 227.
[5] W.L. Brown, W.M. Augustyniak, K.J. Marcantonio, E.H. Simmons, J.W. Boring, R.E. Johnson, C.T. Reimann, Nucl. Instrum. Meth. B 1 (1984) 307.
[6] K.M. Gibbs, W.L. Brown, R.E. Johnson, Phys. Rev. B 38 (1988) 11001.
[7] M.A. Bolorizadeh, M.E. Rudd, Phys. Rev. A 33 (1986) 888.
[8] S.M. Ritzau, R.A. Baragiola, Phys. Rev. B 58 (1998) 2529.
[9] R.E. Johnson, B. Sundqvist, P. Håkansson, A. Hedin, M. Salehpour, G. Såve, Surf. Sci. 179 (1987) 187.
[10] E.M. Bringa, R.E. Johnson, Nucl. Instrum. Meth. B180 (2001) 99.
[11] E.J. Sternglass, Phys. Rev. 108 (1957) 1.
[12] A. Mozumder, J.A. LaVerne, J. Phys. Chem. 89 (1985) 930.
[13] W.O. Hofer, in: R. Behrisch, K. Wittmaack (Eds.), Sputtering by Particle Bombardment III, Springer Verlag, Berlin, 1991.
[14] R.E. Johnson, in: B. Schmitt, C. de Bergh, M. Festou (Eds.), Solar System Ices, Kluwer, Dordrecht, 1998, p. 303.